The Plant Journal (2006) **47**, 687–700 doi: 10.1111/j.1365-313X.2006.02830.x

Visualization of PtdIns3*P* dynamics in living plant cells

Joop E.M. Vermeer[1,3], Wessel van Leeuwen[2], Rafa Tobeña-Santamaria[2], Ana M. Laxalt[4], David R. Jones[5], Nullin Divecha[5], Theodorus W.J. Gadella Jr[1,3,*] and Teun Munnik[2,*]

[1]*Section of Molecular Cytology, Swammerdam Institute for Life Sciences, University of Amsterdam, Kruislaan 316, Amsterdam, The Netherlands,*

[2]*Section of Plant Physiology, Swammerdam Institute for Life Sciences, University of Amsterdam, Kruislaan 318, Amsterdam, The Netherlands,*

[3]*Centre for Advanced Microscopy, Swammerdam Institute for Life Sciences, University of Amsterdam, Kruislaan 318, Amsterdam, The Netherlands,*

[4]*Instituto de Investigaciones Biológicas, Facultad de Ciencas Exactas y Naturales, Universidad Nacional de Mar del Plate, Mar del Plata, Argentina, and*

[5]*Division of Cellular Biochemistry, The Netherlands Cancer Institute, Amsterdam, The Netherlands*

Received 30 January 2006; revised 3 May 2006; accepted 10 May 2006.
[*]For correspondence (fax +31 205 25 6271; e-mail gadella@science.uva.nl and fax +31 205 25 7734; e-mail munnik@science.uva.nl).

Summary

To investigate PtdIns3*P* localization and function in plants, a fluorescent PtdIns3*P*-specific biosensor (YFP–2xFYVE) was created. On lipid dot blots it bound specifically and with high affinity to PtdIns3*P*. Transient expression in cowpea protoplasts labelled vacuolar membranes and highly motile structures undergoing fusion and fission. Stable expression in tobacco BY-2 cells labelled similar motile structures, but labelled vacuolar membranes hardly at all. YFP–2xFYVE fluorescence strongly co-localized with the pre-vacuolar marker AtRABF2b, partially co-localized with the endosomal tracer FM4-64, but showed no overlap with the Golgi marker STtmd–CFP. Treatment of cells with wortmannin, a PI3 kinase inhibitor, caused the YFP–2xFYVE fluorescence to redistribute into the cytosol and nucleus within 15 min. BY-2 cells expressing YFP–2xFYVE contained twice as much PtdIns3*P* as YFP-transformed cells, but this had no effect on cell-growth or stress-induced phospholipid signalling responses. Upon treatment with wortmannin, PtdIns3*P* levels were reduced by approximately 40% within 15 min in both cell lines. Stable expression of YFP–2xFYVE in Arabidopsis plants labelled different subcellular structures in root compared with shoot tissues. In addition labelling the motile structures common to all cells, YFP–2xFYVE strongly labelled the vacuolar membrane in leaf epidermal and guard cells, suggesting that cell differentiation alters the distribution of PtdIns3*P*. In dividing BY-2 cells, YFP–2xFYVE-labelled vesicles surrounded the newly formed cell plate, suggesting a role for PtdIns3*P* in cytokinesis. Together, these data show that YFP–2xFYVE may be used as a biosensor to specifically visualize PtdIns3*P* in living plant cells.

Keywords: yellow fluorescent protein, FYVE domain, lipid signalling, confocal laser scanning microscopy, vesicle trafficking.

Introduction

Polyphosphoinositides (PPIs) are a small group of lipids that function both as signalling molecules and as compartment-specific localization signals for phosphoinositide-binding proteins. One PPI in particular, PtdIns3*P*, has proved to be a crucial player in membrane trafficking events (Corvera *et al.*, 1999; Simonsen *et al.*, 2001; Stenmark and Gillooly, 2001). In the yeast *Saccharomyces cerevisiae*, a single-copy gene, *VPS34*, encodes a phosphatidylinositol-3-kinase (Schu *et al.*, 1993) responsible for the formation of all PtdIns3*P*. VPS34 only uses phosphatidylinositol as substrate, and requires the protein kinase VPS15 for activation and membrane association (Herman *et al.*, 1991; Stack *et al.*, 1995a; Wurmser and Emr, 2002). Yeast cells without a functional VPS34 show a strong defect in vacuolar protein sorting, indicating the importance of PtdIns3*P* in vesicular transport from the *trans*-Golgi to the vacuole (Schu *et al.*, 1993; Stack and Emr, 1994; Stack *et al.*, 1995b; Wurmser and Emr, 1998). Mammalian cells contain three classes of PI3 kinases (Van-

haesebroeck and Waterfield, 1999). Class I PI3Ks are heterodimers consisting of a 110 kDa (p110) catalytic subunit and an adaptor unit. *In vitro*, this class of enzymes uses PtdIns, PtdIns4*P* and PtdIns(4,5)P_2 as substrates, but only the latter is thought to be their preferred substrate *in vivo*, resulting in the formation of PtdIns(3,4,5)P_3. They signal downstream of either tyrosine kinases (class IA) or heterotrimeric G-protein-coupled receptors (class IB) (Vanhaesebroeck and Waterfield, 1999). Class II enzymes are characterized by a C-terminal C2 domain. *In vitro*, these enzymes use PtdIns and PtdIns4*P* as substrates, with the strongest preference for PtdIns (Foster *et al.*, 2003). This class is activated by insulin and integrins, amongst others (Brown *et al.*, 1999; Zhang *et al.*, 1998). Class III enzymes are homologous to the yeast VPS34 and only use PtdIns as substrate. They are probably responsible for most of the PtdIns3*P* synthesis in mammalian cells (Vanhaesebroeck and Waterfield, 1999).

Plants only have a VPS34-type of PI3 kinase (class III). *Arabidopsis thaliana* has one gene (Welters *et al.*, 1994) and homologues have been isolated from *Glycine max*, *Brassica napus* and *Medicago truncatula* (Das *et al.*, 2005; Hernandez *et al.*, 2004; Hong and Verma, 1994). Expression of an antisense *AtVPS34* in Arabidopsis resulted in severe growth defects (Welters *et al.*, 1994), suggesting a crucial role for PtdIns3*P* and its synthesis. PtdIns3*P* levels in plants are relatively low, typically approximately 2–15 % of the PtdIns*P* pool, but turn over rapidly (Meijer *et al.*, 2001; Munnik *et al.*, 1994a,b).

Identification of the FYVE domain has brought new impetus into PtdIns3*P* studies. FYVE was named after the first four proteins found to contain such a domain, namely Fab1p, YOTB, Vac1p and EEA1, and consists of a cysteine-rich region that binds two Zn^{2+} ions and contains a highly characteristic R(R/K)HHCRXCG motif (Corvera *et al.*, 1999; Stenmark *et al.*, 1996). More importantly, it specifically binds PtdIns3*P* (Burd and Emr, 1998; Gaullier *et al.*, 1998, 1999; Kutateladze *et al.*, 1999). Fusion of the FYVE domain to GFP and expression in cells produced the first images of its subcellular distribution (Burd and Emr, 1998; Kutateladze *et al.*, 1999). Meanwhile, it has become an accepted tool to study PtdIns*3P* dynamics in yeast and mammalian cells (Ellson *et al.*, 2001; Gillooly *et al.*, 2000; Parrish *et al.*, 2004). In plant research, the use of such biosensors is still sporadic. Although three reports have described the use of an FYVE domain–GFP chimera to visualize PtdIns3*P*, all studies were conducted in transient systems only (Jung *et al.*, 2002; Kim *et al.*, 2001; Park *et al.*, 2003). Moreover, they used the FYVE domain of *Homo sapiens*, Early Endosomal Antigen1 in combination with its adjacent Rab5-binding region that was shown to be crucial for the observed subcellular localization of this FYVE–GFP chimera.

In this study, YFP was fused to a tandem dimer of the FYVE domain originating from the mouse hepatocyte growth factor-regulated tyrosine kinase substrate, Hrs (Gillooly *et al.*, 2000), which does not contain a Rab5-binding domain. We show that this fusion binds specifically and with high affinity to PtdIns3*P*. Detailed analysis of its expression in three different systems was conducted: transient expression in cowpea protoplasts, and stable expression in tobacco BY-2 cells and *A. thaliana*. All these systems allowed PtdIns3*P* to be visualized in living cells without any obvious detrimental effect of the over-expression of the biosensor.

Results

In vitro *binding of GST–YFP–2xFYVE*

Prior to testing YFP–2xFYVE as a PtdIns3*P* biosensor in plant cells, we first needed to confirm the lipid-binding specificity of the construct. To this end, a GST fusion was expressed in *Escherichia coli* and the purified fusion protein subjected to a protein–lipid overlay assay: a nitrocellulose membrane with various phosphorylated inositol phospholipids spotted at different concentrations. As shown in Figure 1(a), it specifically bound PtdIns3*P*, without cross-reacting with any of the other polyphosphoinositide isomers. GST alone did not give any signal (not shown).

Transient expression of YFP–2xFYVE in cowpea protoplasts

Cowpea (*Vigna unguiculata* L.) protoplasts were transfected with a plasmid containing YFP–2xFYVE under the control of a constitutive promoter (35S) (Figure 1b). Sixteen hours after transfection, YFP–2xFYVE fluorescence was seen as small punctated structures (0.57 ± 0.2 μm, $n = 80$) and also on the vacuolar membrane (Figure 1c,d; two different confocal planar views of the same cowpea protoplast expressing YFP–2xFYVE). The small punctated structures were highly motile (see Supplementary Movie S1). Occasionally (approximately 1%), protoplasts with very high YFP–2xFYVE fluorescence revealed larger vesicular structures, present inside the central vacuole (Figure 1e). In general, the protoplast appearance and viability seemed unaffected by the expression of YFP–2xFYVE compared with protoplasts expressing unfused YFP.

Expression of YFP–2xFYVE in stable transformed BY2 cells

The advantage of the transient protoplast system is that the expression of YFP constructs can be quickly assessed. A limitation, however, is that protoplasts undergo excessive cell wall regeneration and are physiologically stressed (J.E.M. Vermeer, J. Goedhart, W. van Leeuwen, T. Munnik, T.W.J. Gadella Jr, unpublished results). Hence, they are not ideal to monitor PtdIns3*P* dynamics *in vivo* in response to a stimulus. Therefore, stably trans-

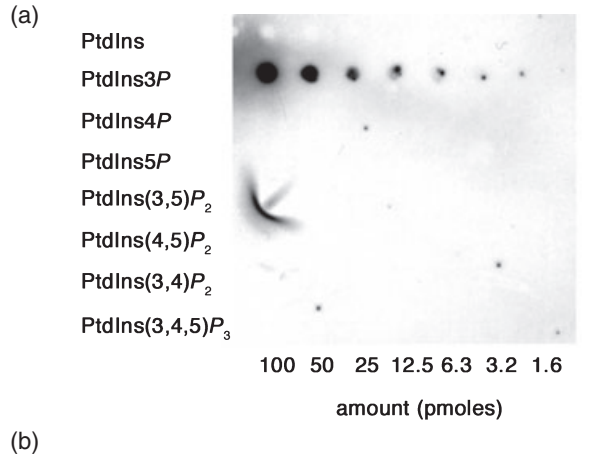

Figure 1. YFP–2xFYVE: *in vitro* lipid binding and expression in cowpea protoplasts.
(a) Protein–lipid overlay of GST–YFP–2xFYVE to determine the phospholipid-binding specificity of YFP–2xFYVE *in vitro*. All naturally occurring polyphosphoinositides were spotted onto a nylon membrane in a concentration range from 1.6–100 pmol. Binding was detected using an anti-GST antibody.
(b) Schematic overview of the PtdIns*3P* biosensor YFP–2xFYVE, used in transient and stable expression studies.
(c,d) Two different confocal planes of a cowpea protoplast transiently expressing YFP–2xFYVE, showing the vacuolar membrane in the medial section (c) and punctated structures labelled by YFP–2xFYVE in the basal section (d) of the same protoplast.
(e) Protoplast highly expressing YFP–2xFYVE showing large vesicles present inside the central vacuole.
For images (c)–(e): left panel, YFP fluorescence; middle panel, chlorophyll autofluorescence; right panel, differential interference contrast. Bar = 10 μm.

formed tobacco BY-2 cells expressing YFP–2xFYVE were generated. As a control, BY-2 cells were transformed with a plasmid containing YFP only. Both cell lines were

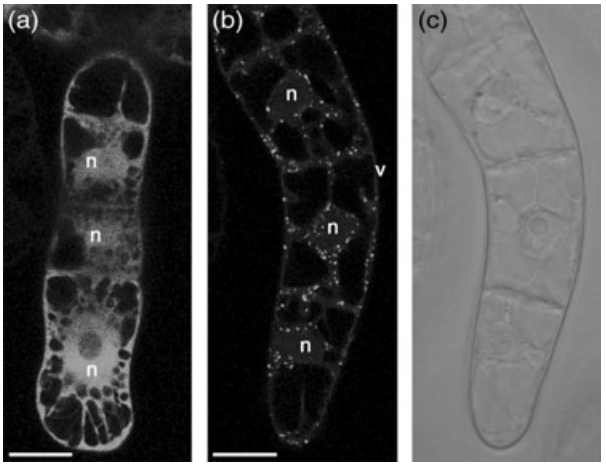

Figure 2. Confocal images of BY-2 cells expressing unfused YFP (a) or YFP–2xFYVE (b,c), of which (b) YFP fluorescence and (c) differential interference contrast image. n, nucleus; v, vacuolar membrane. Bar = 10 μm. See also Supplementary Movie S2.

identical in appearance to untransformed BY-2 cells and grew normally (not shown).

While the fluorescence of the control cells was present throughout the cytosol and the nucleus (Figure 2a), the BY-2 cells expressing YFP–2xFYVE revealed numerous punctated structures (Figure 2b) that were rapidly moving, resembling the structures observed in cowpea protoplasts (Figure 1c,d). These vesicle-like structures were of two different sizes: smaller, 0.47 ± 0.10 μm ($n = 100$), and larger vesicles, 1.18 ± 0.29 μm ($n = 100$). All labelled vesicles were excluded from the nucleus (see Supplementary Movie S2). In contrast to the cowpea protoplasts, only faint labelling of the vacuolar membrane was observed in YFP–2xFYVE BY-2 cells.

Next, the dynamics and characteristics of the YFP–2xFYVE-labelled vesicles were examined. This was performed by studying subsequent images taken from a time series (Figure 3; Supplementary Movie S3). Most YFP–2xFYVE-labelled vesicles were moving, displaying 'kiss and run' behaviour (Duclos *et al.*, 2000), although some were found to be stationary for a while before moving out of the focal plane (arrowheads, Figure 3). In addition to 'kiss and run' behaviour, YFP–2xFYVE-labelled vesicles also appeared to fuse with (Figure 3, circles) and separate from each other (Figure 3, squares). The fusion events seemed to be limited to the larger vesicles; the smaller appeared to remain single.

To determine whether movement of the YFP–2xFYVE-labelled vesicles depended on the actin or the microtubular cytoskeleton, two different drugs were used: latrunculin A (1 μM), to disrupt the actin cytoskeleton, and oryzalin (10 μM), a microtubule-depolymerizing agent. While oryzalin

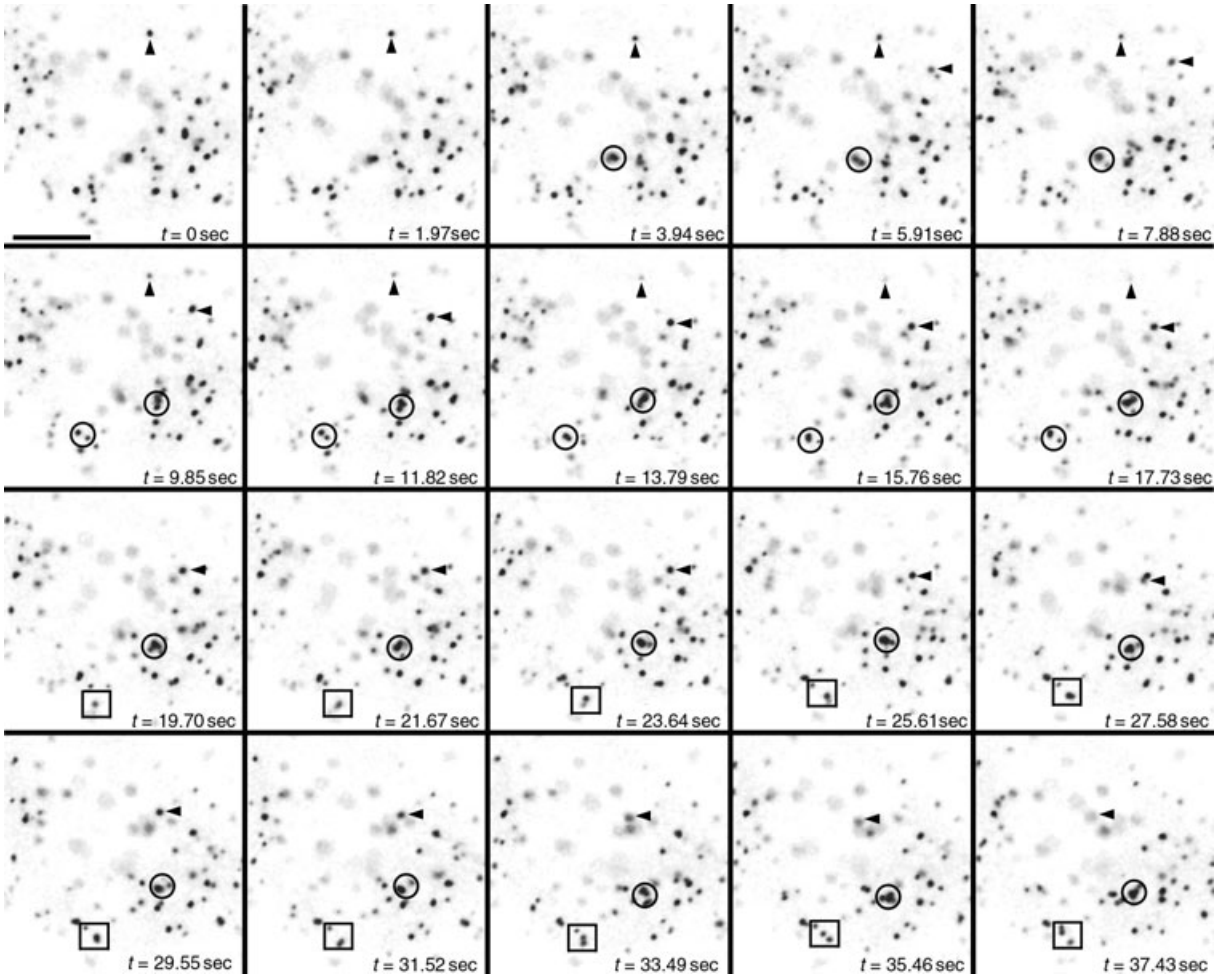

Figure 3. Dynamics and characteristics of YFP–2xFYVE-labelled vesicles.
Sequential confocal images taken at 1.97 sec intervals, revealing movement, fusion and fission events. Arrowheads indicate stationary vesicles. Circles indicate vesicles that appear to merge with each other. Squares indicate vesicles that first appear to merge and then separate again approximately 8 sec later into two smaller vesicles. The images are part of Supplementary Movie S3. Bar = 10 μm, time (*t*) is indicated. The total image comprises an area 28 by 28 μm of a single cell.

had no effect on the dynamics of the YFP–2xFYVE-labelled vesicles, latrunculin A completely arrested all movement (Supplementary Movies S4 and S5). These results suggest that YFP–2xFYVE-labelled vesicles are transported via the actin cytoskeleton.

Effects of the PI3 kinase inhibitor wortmannin on YFP–2xFYVE-labelled vesicles

Wortmannin is a potent inhibitor of PI3 kinase activity, inhibiting the phosphorylation of phosphatidylinositol to PtdIns3*P* (Arcaro and Wymann, 1993; Stephens *et al.*, 1994). To determine its effect on YFP–2xFYVE labelling, cells were treated with 10 μM wortmannin and followed in time. As shown in Figure 4(a), within minutes of adding wortmannin, the YFP–2xFYVE label disappeared from the vesicles and simultaneously appeared in the cytosol and nucleus (see Supplementary Movie S6). After 15–20 min, most of the YFP–2xFYVE fluorescence was in the cytosol and nucleus. After 1–2 h, labelling reappeared on membrane structures, but now vesicles appeared larger (Figure 4c). Wash-out of the wortmannin resulted in relocalization of the YFP–2xFYVE fluorescence onto the vesicular structures, just as in untreated cells (data not shown). However, wortmannin is labile in water, so it is also possible that the reversible effect of is due to newly synthesized proteins escaping the inhibition.

These results suggest that wortmannin reduces the PtdIns3*P* levels in the vesicles, and, as a result, the YFP–2xFYVE sensor is released and diffuses throughout the cytosol and into the nucleus. The accumulation of YFP–2xFYVE fluorescence in the nucleus seemed to be the result of active transport, as its fluorescence was often much higher than in the cytosol (Figure 4).

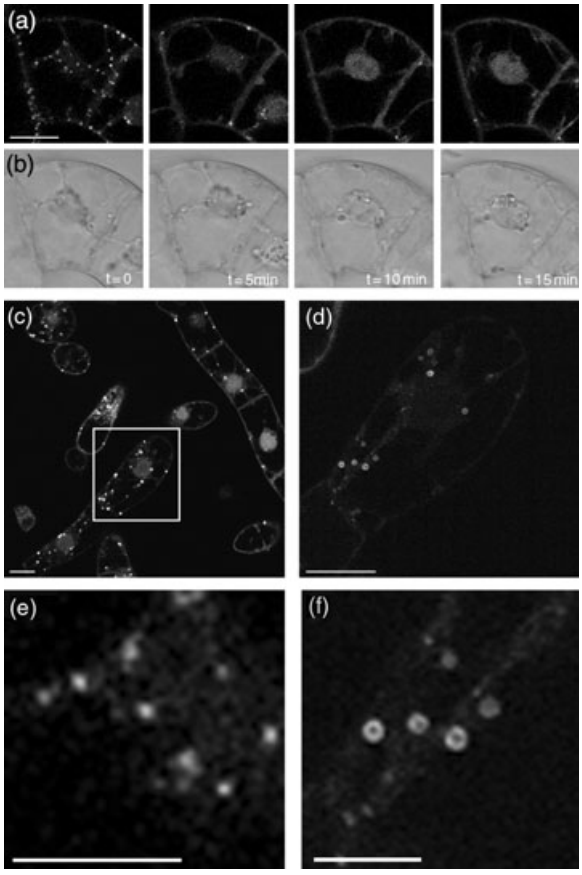

Figure 4. Effects of the PtdIns-3 kinase inhibitor wortmannin on the localization of YFP–2xFYVE in BY-2 cells.
(a,b) Consecutive confocal fluorescence images of YFP–2xFYVE-expressing cells after the addition of 10 μM wortmannin at $t = 0$; (a) YFP–2xFYVE fluorescence, (b) differential interference contrast image. Fluorescence gradually disappears from the vesicles and becomes distributed throughout cytoplasm and nucleus.
(c) Confocal fluorescence image of YFP–2xFYVE cells 1.5 h after the addition of 10 μM wortmannin, showing the appearance of larger vesicles.
(d) Magnification taken from the boxed area shown in (c) taken with lower laser intensity to reveal the vesicular shape of the YFP–2xFYVE-labelled structures.
(e,f) Magnification of vesicles before (e) and after (f) long wortmannin treatment.
Bar in (a–d) = 10 μm; bar in (e,f) = 5 μm. See also Supplementary Movie 6.

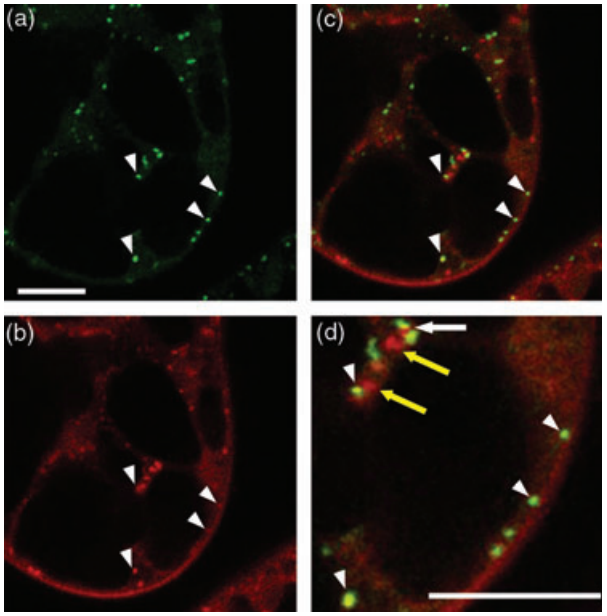

Figure 5. YFP–2xFYVE-labelled vesicles partly co-label with the endosomal tracer FM4-64.
Confocal fluorescence image of YFP–2xFYVE cells pulse-labelled (10 min) with FM4-64 (4 μM). (a) YFP fluorescence, (b) FM4-64 fluorescence, (c) overlay. (d) Magnification of an area from (c). Arrowheads show co-labelling of vesicles with YFP–2xFYVE and FM4-64 vesicles; white arrow indicates partial overlap between YFP–2xFYVE and FM4-64. Yellow arrows indicate labelling of vesicles by FM4-64 only. Bars = 10 μm.

YFP–2xFYVE labels endocytic/pre-vacuolar vesicles

In yeast and mammalian cells, PtdIns3*P* is mainly localized in endocytic compartments (Burd and Emr, 1998; Gaullier *et al.*, 1998; Gillooly *et al.*, 2000). To investigate its location in plant cells, YFP–2xFYVE cells were incubated with the styryl dye FM4-64, which is a commonly used endocytic tracer in plant cell studies (Bolte *et al.*, 2004; Meckel *et al.*, 2004; Parton *et al.*, 2003; Takano *et al.*, 2005; Zheng *et al.*, 2005). Figure 5 (and Supplementary Movie S7) shows a representative picture, after a 10 min pulse labelling with 4 μM FM4-64. Typically, only approximately 10–20% of the YFP–2xFYVE-labelled vesicles were co-labelled with FM4-64 (arrowheads in Figure 5). Sometimes, partial co-labelling was observed (arrow in Figure 5). To further investigate the identity of the YFP–2xFYVE-labelled vesicles, BY-2 cells were co-transformed with YFP–2xFYVE and either mRFP–AtRabF2b (Ara7), an endosomal/pre-vacuolar marker (Kotzer *et al.*, 2004; Lee *et al.*, 2004; Ueda *et al.*, 2001), or with STtmd–CFP, a Golgi marker (Boevink *et al.*, 1998). Most of the YFP–2xFYVE-labelled vesicles were found to co-localize with mRFP–AtRabF2b (Figure 6a–d; Supplementary Movie S8). In contrast, there was no co-labelling of YFP–2xFYVE-labelled vesicles and STtmd–CFP-labelled Golgi stacks (Figure 6e–h; Supplementary Movie S9). Frequently, however, YFP–2xFYVE-labelled vesicles appeared in close proximity to the STtmd–CFP-labelled Golgi stacks, suggesting a possible transient interaction between the two.

YFP–2xFYVE-expressing cells exhibit a normal stress response, but have a twofold higher PtdIns3P level

As mentioned earlier, YFP–2xFYVE cells exhibited no apparent phenotype. However, as YFP–2xFYVE labelled endocytic/pre-vacuolar vesicles, and endocytic transport is involved in various plant signalling processes, e.g. auxin

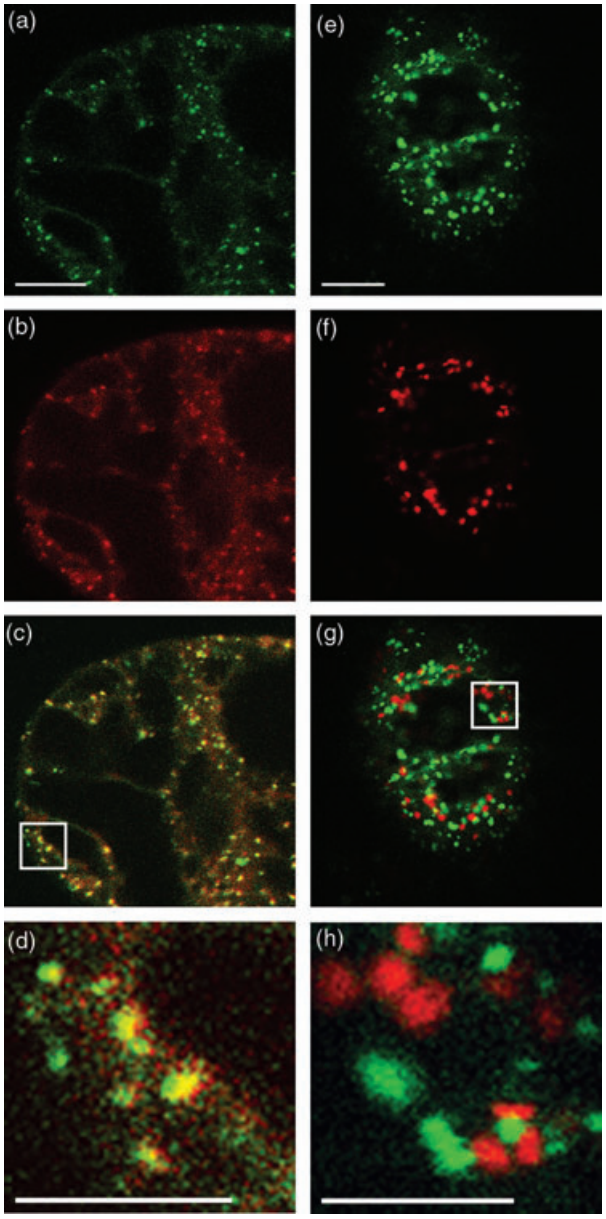

Figure 6. Co-labelling of YFP–2xFYVE-labelled structures with endosomal and Golgi markers.
Confocal fluorescence images of BY-2 cells co-expressing (a–d) YFP–2xFYVE (green) and the endosomal/pre-vacuolar marker mRFP–AtRABF2b (red) and (e–h) YFP–2xFYVE and the Golgi marker STtmd–CFP (red). (a) YFP–2xFYVE, (b) mRFP–AtRABF2b, (c) overlay, (d) close-up of boxed area of (c), showing co-labelling between YFP–2xFYVE and mRFP–AtRABF2b, (e) YFP–2xFYVE, (f) STtmd–CFP, (g) overlay, (h) close-up of boxed area of (g), showing that there is no co-localization between YFP–2xFYVE and STtmd–CFP, although the structures are in close proximity to each other. Bars (a–c,e–g) = 10 μm; bars in (d,h) = 5 μm.

transport (Paciorek *et al.*, 2005), we wished to determine whether over-expressing the PtdIns3*P* biosensor affected the lipid content and associated signalling. To this end, $^{32}P_i$-radiolabelling studies on untransformed, YFP- and YFP–2xFYVE-transformed BY2 cells were conducted. To activate different lipid signalling pathways, cells were osmotically stressed (250 mM NaCl; 15 min) or treated with mastoparan (5 μM Mas7; 15 min). A typical response to hyper-osmotic stress is an increase in PtdIns(4,5)P_2 (DeWald *et al.*, 2001; Pical *et al.*, 1999), while Mas7, a potent activator of PLC and PLD signalling pathways, results in the formation of phosphatidic acid and diacylglycerolpyrophosphate (Frank *et al.*, 2000; van Himbergen *et al.*, 1999; Munnik *et al.*, 1998). As shown in Figure 7(a), untransformed, YFP- and YFP–2xFYVE-transformed BY2 cells exhibited very similar radiolabelled phospholipid pools and showed identical responses to salt and mastoparan. Also lower concentrations of salt produced no differences (Figure 7b,c). Hence, the transgenes did not seem to interfere with lipid signalling.

To further analyse the PtdIns3*P* content of these cells, HPLC headgroup analyses were performed. Strikingly, YFP–2xFYVE cells were found to have a twofold higher PtdIns3*P* level than the YFP cells (Figure 7d). As a percentage of total phospholipids, YFP cells contained 0.37% ± 0.13 ($n = 4$) PtdIns3*P* as opposed to 0.73% ± 0.20 ($n = 4$) PtdIns3*P* in YFP–2xFYVE-transformed cells. Treatment with 10 μM wortmannin reduced the PtdIns3*P* contents by almost 40% within 15 min in both cell lines (38% ± 9, $n = 4$ for YFP cells and 39% ± 7, $n = 4$, for YFP–2xFYVE cells). The levels of PtdIns4*P* (approximately 10% of the total) hardly changed after the cell treatments.

Expression of YFP–2xFYVE in A. thaliana

To investigate whether such a biosensor can be used in whole plants, transgenic Arabidopsis plants stably expressing YFP–2xFYVE were generated. Of the two lines generated, homozygous T_3 lines grew normally and were indistinguishable from YFP-transformed or untransformed plants (data not shown). As shown in Figure 8, YFP–2xFYVE was expressed throughout the plant and was localized on small, highly motile vesicles and sometimes also on vacuolar membranes. The vesicles were similar to those observed in BY-2 cells and could also be divided into smaller (0.57 ± 0.11 μm, $n = 75$) and larger (1.02 ± 0.2 μm, $n = 75$) populations. In root cortical cells, YFP–2xFYVE fluorescence was only observed on small vesicles (Figure 8b,c). In older root epidermal cells, vacuolar membranes were also labelled (Figure 8d,e). In the tip area of growing root hairs, many rapidly moving vesicles were observed (Figure 8h,i and Supplementary Movie S10). In leaf epidermal and guard cells, YFP–2xFYVE fluorescence was present on motile vesicular structures, but also strongly present on the vacuolar membrane (Figure 8m–p; Supplementary Movies S11–S14). Stomata often had large labelled vesicles (2–5 μm) inside the central vacuole, resembling structures also occasionally observed in cowpea protoplasts.

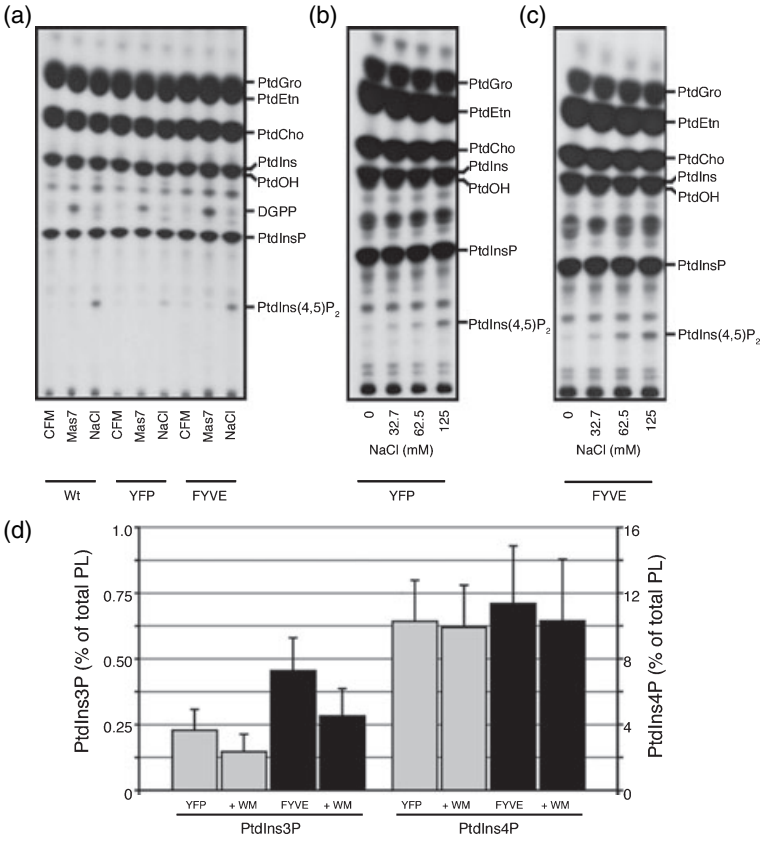

Figure 7. Phospholipid composition in untransformed (wild-type, Wt) BY-2 cells and those expressing YFP or YFP–2xFYVE (FYVE).
(a) Cells were labelled for 3 h with $^{32}P_i$ and then incubated for 15 min with cell-free medium (CFM) with or without 250 mM NaCl or 5 μM Mas7.
(b,c) Responses in YFP (b) or FYVE (c) cells to increasing NaCl concentrations.
(d) HPLC analysis of PtdIns3*P* and PtdIns4*P* levels in YFP and YFP–2xFYVE cells with or without treatment with 10 μM wortmannin (WM). PL, phospholipid levels.

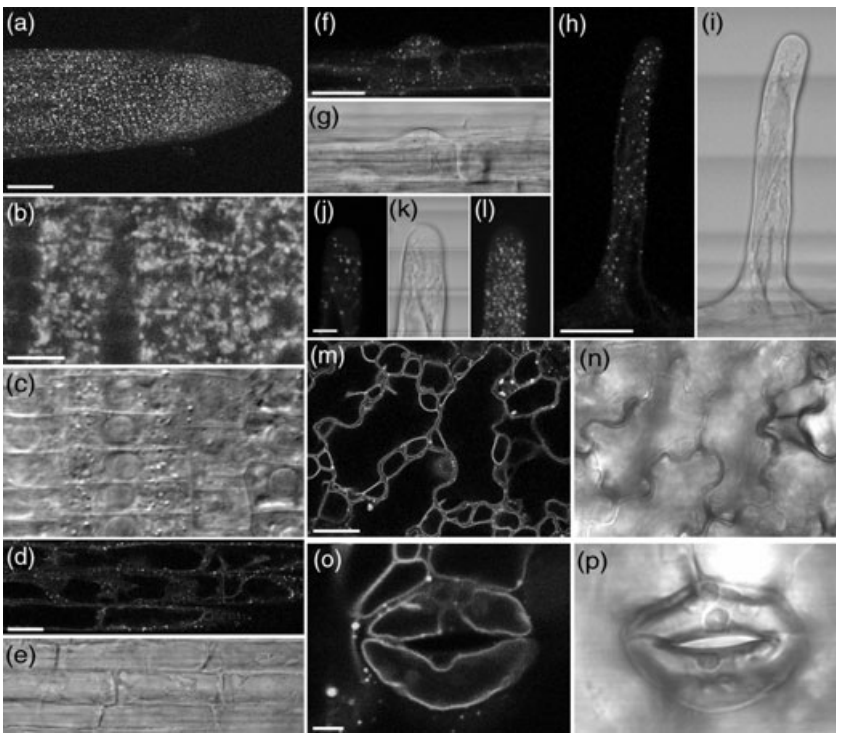

Figure 8. YFP–2xFYVE expression in *Arabidopsis* plants.
Confocal fluorescence images taken from different cell types from Arabidopsis plants stably expressing YFP–2xFYVE. Maximal projection of an image stack taken from (a) a root tip, (b,c) root cortex cells, (d,e) root epidermal cells, (f,g) bulging root hair, and (h,i) growing root hair. (j,k) High magnification of the tip of a growing root hair, and (l) maximal projection of the growing root hair shown in (j,k), (m,n) leaf epidermal cells and (o,p) guard cells. Bars = (a) 50 μm, (b, d) 10 μm, (f,h,m) 20 μm and (j,o) 5 μm. Images (a, b, d, f, h, j, l, m and o) show YFP fluorescence, while (c, e, g, i, k, n and p) show differential interference contrast images.

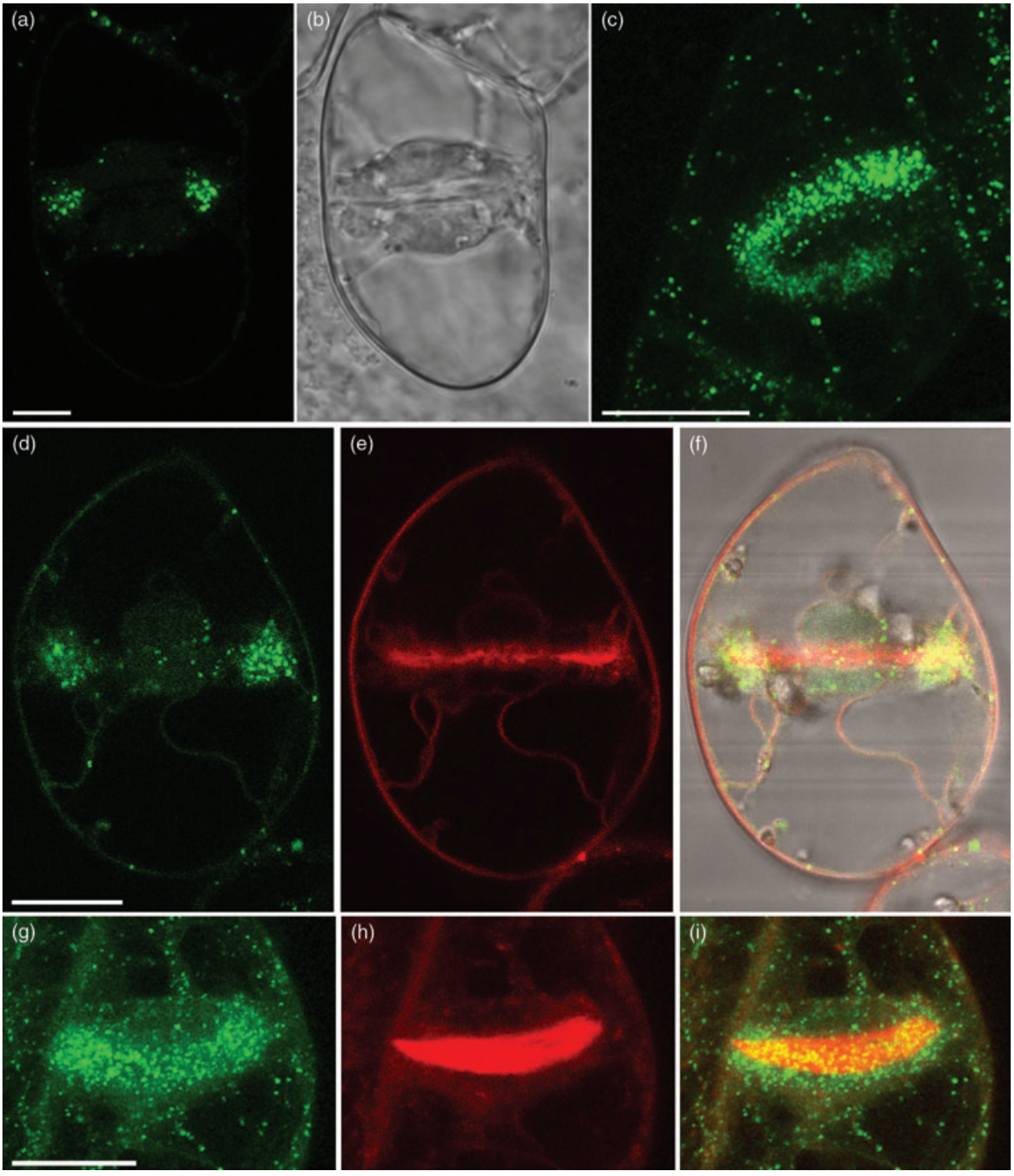

Figure 9. YFP–2xFYVE-labelled vesicles accumulate around the expanding cell plate in a dividing BY-2 cell.
(a,b) Confocal image of a dividing BY-2 cell expressing YFP–2xFYVE; (a) YFP fluorescence, (b) differential interference contrast image.
(c) Projection of an image stack of a dividing cell.
(d–i) Dividing YFP–2xFYVE cell co-labelled with the endocytic tracer FM4-64 (4 μM): (d–f) confocal medial plane, (g–i) maximal image projection of an image stack; (d,g) YFP fluorescence, (e,h) FM4-64 fluorescence, (i,h) overlay. Bars = 10 μm.

PtdIns3P dynamics during cytokinesis in BY-2 cells

When analysing YFP–2xFYVE-transformed cells, we occasionally observed cells that were in the middle of the process of division. In such cells, PtdIns3*P*-containing vesicles strongly accumulated at the growing edges of the newly formed cell plate (Figure 9a–c; Supplementary Movies S15 and S16). A maximal projection of an image stack of a

dividing YFP–2xFYVE-transformed cell is depicted in Figure 9(c). It shows that the PtdIns3*P*-containing vesicles completely surround the newly formed cell plate as a ring, but, importantly, did not label the cell plate itself.

Earlier, FM4-64 had been shown to be rapidly internalized into newly formed cell plates (Bolte *et al.*, 2004; Dhonukshe *et al.*, 2006). When FM4-64 was added and dividing cells analysed (Supplementary Movies S17 and S18), a clear cloud of PtdIns3*P* vesicles was visible as a belt, surrounding the newly formed FM4-64-labelled cell plate (Figure 9e–j). These results suggest that PtdIns3*P* is involved in transport of vesicles to the new cell membrane, but is itself excluded from it.

Discussion

Using YFP–2xFYVE as a PtdIns3P biosensor

The use of a 2xFYVE domain fused to YFP has been described to study the localization and dynamics of PtdIns3*P*-containing structures in living plant cells. A tandem dimer of the FYVE domain of Hrs was used, which was shown to be specific for PtdIns3*P* (Gillooly *et al.*, 2000; this work). Three different plant systems were used: (i) transient expression in cowpea protoplasts, and stable expression in (ii) tobacco BY-2 cells and (iii) Arabidopsis plants. The FYVE domain has been used previously to monitor PtdIns3*P* in plant cells. These studies used the transient expression of GFP–EBD in Arabidopsis protoplasts and guard cells (Jung *et al.*, 2002; Kim *et al.*, 2001; Park *et al.*, 2003). GFP–EBD consists of the FYVE domain of the human early endosome antigen-1 but also a binding region for Rab5, a small G-protein involved in vesicle trafficking (Kim *et al.*, 2001; Zerial and McBride, 2001; Zerial and Stenmark, 1993). GFP–EBD was localized on various compartments such as Golgi stacks, the pre-vacuolar compartment, the vacuolar membrane and vesicles within the central vacuole. Importantly, this study revealed that, in addition to the FYVE domain, the Rab5-binding region was essential for labelling of the vesicles by GFP–EBD. Hence, as this probe binds Rab5 too, it is difficult to argue that GFP–EBD specifically labels PtdInd3*P*-containing membranes.

In contrast, the YFP–2xFYVE chimera is a genuine PtdIns3*P* biosensor as has also been shown for nematodes, yeast and mammalian cells (Gillooly *et al.*, 2000; Henry *et al.*, 2004; Roggo *et al.*, 2002). It binds PtdIns3*P* itself (Figure 1a), and, *in planta*, YFP–2xFYVE is sensitive to the PI3 kinase inhibitor wortmannin. Within 15 min of treatment, the YFP–2xFYVE fluorescence disappeared from the membrane vesicles and reappeared in the cytosol and nucleus (Figure 4). Using $^{32}P_i$-labelling and HPLC headgroup analysis, wortmannin was shown to reduce the PtdIns3P pool by more than one-third within 15 min, confirming that PtdIns3P is turning over rapidly, as has been found previously for mammalian cells and the green alga *Chlamydomonas* (Munnik *et al.*, 1994a,b; Stephens *et al.*, 1989). The effect of wortmannin was more apparent on the YFP–2xFYVE-labelled vesicles than that on the $^{32}P_i$-labelled PtdIns3*P* pool. The remaining part of the $^{32}P_i$-labelled PtdIns3*P* pool is most likely occupied by endogenous PtdIns3*P* targets. The genome of Arabidopsis is predicted to contain 16 proteins with a predicted FYVE domain and another 11 with a PX domain, which is also known to bind PtdIns3*P* (van Leeuwen *et al.*, 2004). HPLC analysis of the $^{32}P_i$-labelled PtdIns3*P* pool showed that YFP–2xFYVE-transformed cells contained twice as much PtdIns3*P* as YFP cells. However, cells responded similarly to stress and did not exhibit a phenotype (Figure 7a–c). The most simple mechanistic explanation is that YFP–2xFYVE effectively titrates away some of the PtdIns3*P* pool, in response to which the PI3 kinase maintains an unaltered freely accessible pool of PtdIns3*P*. We did not measure PtdIns3*P* levels in Arabidopsis plants expressing YFP–2xFYVE, but they also showed no phenotype, and displayed good fluorescence labelling throughout the plant (Figure 8).

Identity of PtdIns3P-containing membranes

In BY-2 cells, co-localization experiments with YFP–2xFYVE and the endocytic tracer FM4-64 showed a partial overlap (Figure 5), suggesting that some of the YFP–2xFYVE-labelled vesicles could be endosomes. Double transformations with YFP–2xFYVE and an Arabidopsis Rab5 homologue, At-RABF2b, showed strong co-localization (Figure 6a–d), whereas no co-localization was observed with YFP–2xFYVE and the Golgi marker STtmd–CFP (Figure 6e–h). Also in mammalian cells, PtdIns3*P*-containing vesicles co-localize with Rab5 (Shin *et al.*, 2005), and, in yeast, PtdIns3*P* is involved in vesicular trafficking from the late Golgi to the vacuole (Herman and Emr, 1990). This could also be the case in plants, as PtdIns3*P* is present both in endosomal/pre-vacuolar vesicles and vacuolar membranes, and YFP–2xFYVE-labelled vesicles were frequently observed in close proximity to Golgi stacks (Figure 6h). In support of this, transient interactions between AtRABF2b and Golgi (STtmd–CFP-labelled) stacks have recently been described (Dhonukshe *et al.*, 2006).

In Arabidopsis, leaves and stomata showed strong fluorescent labelling of vacuolar membranes, and contained small motile structures, similar to those observed in BY-2 cells. Although no co localization experiments were performed, it seems likely that they represent endosomal and pre-vacuolar vesicles of Arabidopsis. The different levels of vacuolar membrane labelling with YFP–2xFYVE between root, epidermal leaf cells and stomata could be due to their different states of differentiation.

The large vesicles observed inside the central vacuoles of stomata (which were also observed in cowpea protoplasts with high expression of YFP–2xFYVE) resemble the vesicles

observed in Arabidopsis guard cells using transient expression (Jung *et al.*, 2002; Park *et al.*, 2003). We think that these structures might be autophagosomes. Autophagy is a process in which cytosol and organelles are sequestered within double-membrane structures that deliver the contents to the lysosome/vacuole for degradation (Klionsky, 2005). In yeast, PI3 kinase is required for autophagy (Kihara *et al.*, 2001), and there are several autophagosomal proteins that bind PtdIns3*P* (Stromhaug *et al.*, 2004; Wurmser and Emr, 2002). Arabidopsis contains proteins homologous to several of these yeast autophogosomal proteins, and they have recently been shown to be required for autophagosome function and localization (Contento *et al.*, 2005; Xiong *et al.*, 2005).

A possible role for PtdIns3P during cytokinesis?

A recent report from Dhonukshe *et al.* (2006) showed that endocytosis of cell surface material mediates cell plate formation during cytokinesis (Dhonukshe *et al.*, 2006). In dividing BY-2 cells, PtdIns3*P*-containing vesicles were found to surround the newly formed FM4-64-labelled cell plate as a belt. More importantly, YFP–2xFYVE fluorescence was excluded from the newly formed membrane, indicating that there was no, or hardly any, PtdIns3*P* present. Although YFP–2xFYVE partially co-localized with FM4-64 (Figure 5), this did not occur at the cell plate. If the PtdIns3*P*-containing vesicles fuse with the cell plate, why is there no labelling of the cell plate? Three potential explanations exist. First, PtdIns3*P* may be dephosphorylated by a PtdIns*3P*-specific phosphatase. The Arabidopsis genome is predicted to contain two myotubularin homologues, which are phosphatases that have been shown to act on PtdIns3*P* in yeast and animal cells (Blondeau *et al.*, 2000; Clague and Lorenzo, 2005; Parrish *et al.*, 2005; Taylor *et al.*, 2000). Alternatively, PtdIns3*P* may be phosphorylated by a PtdIns3*P* 5-kinase into PtdIns(3,5)P_2. *Arabidopsis* contains four putative PtdIns3*P* 5-kinases, of which two contain a FYVE domain (van Leeuwen *et al.*, 2004), and plants do make PtdIns(3,5)P_2 (Meijer *et al.*, 1999). Finally, PtdIns3*P* may be actively recycled to a so-far unidentified compartment, e.g. pre-vacuolar structures.

The role of PtdIns3*P* during cytokinesis may also explain the observation that Arabidopsis plants expressing an antisense *AtVPS34* show a severe growth phenotype (Welters *et al.*, 1994), and that wortmannin inhibits cell plate growth (Dhonukshe *et al.*, 2006). In addition, Dhonukshe *et al.* (2006) showed enlargement of GFP–AtRABF2b-labelled and FM4-64-labelled vesicles after 15 min treatment with wortmannin. These structures closely resembled those labelled by YFP–2xFYVE after prolonged wortmannin treatment (Figure 4d). This suggests that PI3 kinase and its product PtdIns3*P* are involved in late endosomal transport processes downstream from endocytic vesicles in plants. The observations made in this study, those by Dhonukshe *et al.* (2006) and the studies by Kim using GFP–EBD are all consistent with the hypothesis that the PtdIns3*P*-labelled structures identify a late endosomal compartment receiving material from both the early endocytic and Golgi pathways for simultaneous delivery to the growing cell plate. Given the future destiny of the cell plate as plasma membrane, one can also consider the structure as a recycling endosome (Behnia and Munro, 2005). The close association, but lack of co-localization with Golgi stacks, suggests that Golgi-derived material enters the PtdIns3*P*-labelled structures by short-range vesicle transport. The swollen structures after prolonged wortmannin treatment could indicate that forward delivery (fission of vesicles with destiny) to the cell plate requires PtdIns3*P*. This hypothesis implies that spatial control of PtdIns3*P* synthesis and breakdown is a key event in regulating cell plate growth during cytokinesis.

In *S. cerevisiae*, VPS34 requires the protein kinase VPS15 for its activity and is probably also responsible for targeting the soluble VPS34 to membranes (Herman and Emr, 1990; Herman *et al.*, 1991). Although Hong and Verma (1994) showed that soybean PI3 kinase activity was associated with membrane proliferation in young nodules (Hong and Verma, 1994), not much is known about where PI3 kinase resides and how its activity is regulated. Arabidopsis has a putative orthologue of ScVPS15 (Mueller-Roeber and Pical, 2002), which makes it possible that a similar complex exists. The use of lipid-binding domains fused to fluorescent proteins in combination with PI3 kinase–GFP fusions and PI3 kinase mutants will be useful to tackle this process further.

Experimental procedures

Constructs

Constructs were made using standard molecular biological methods. To create pGreen35S::YFP–2xFYVE, the tandem fusion of the FYVE domain of mouse Hrs was amplified from the plasmid pGEM-myc–2xFYVE$_{Hrs}$, (kindly provided by Dr H. Stenmark, The Norwegian Radium Hospital, Oslo, Norway) using the following primers: XhoI-FYVEfwd 5′-CCGCTCGAGTGAATTTATCAATTGAATTC-GAAAGTG-3′ and BclHP2FYVErev 5′-CCGTGATCAATAGAATACAA-GCTTGGGCTGCAG-3′. The 0.5 kb fragment was transferred to *Xho*I- and *Bam*HI-digested pGreen-1K-EYFP, with the additional Q69K mutation to decrease pH stability, containing a double CaMV 35S promoter and an *NPTII* gene for selection. To generate pMON35S::YFP–2xFYVE, a 0.8 kb *Eco*RI- and *Sma*I-digested 2-xFYVE and nos terminator-containing fragment was transferred to *Eco*RI- and *Sma*I-digested pMONd35S::sYFP2. For double transformations, the YFP–2xFYVE Tnos fragment was transferred to pBIN+d35S using *Xba*I and *Sma*I, yielding pBIN+d35S::YFP–2xFYVE. The Golgi marker pMONd35S::STtmd–CFP was created by exchanging YFP for CFP in pMONd35S::STtmd–YFP, kindly provided by Dr J. Carette (Wageningen University, The Netherlands), using *Nco*I and *Bam*HI. To create pCambiad35S::STtmd–CFP, the d35S::STCFP–Tnos cassette was released from pMONd35S::STtmd–CFP using *Hin*dIII and *Sma*I and transferred to pCambia1390 digested with *Hin*dIII and *Sma*I. The endosomal marker

pMONd35S::mRFP–AtRABF2b (ARA7) was created by amplifying ARA7 from pHTSB-GFP–ARA7, kindly provided by Dr A. Nakano (RIKEN, Tokyo, Japan), using the following primers: JV-ARA7Accfw 5′–CATGTCCGGAGGATCTGGAGCTGCAGCTGGAAACAAG-3′ and JV-ARA7TbamHI 5′-CGGGATCCCTAAGCACAACAAGATGAG-3′. Subsequently, the fragment was transferred to pmRFPc1, using *Acc*III and *Bam*HI. The mRFP–ARA7 fusion was transferred using *Nhe*I and *Bam*HI to pMON999d35S digested with *Xba*I and *Bam*HI. The d35S::mRFP–AtRABF2b–Tnos cassette was transferred to pCambia1390 using *Hin*dIII and *Sma*I. The mRFP was kindly provided by Dr R.Y. Tsien, (University of California, San Diego, CA, USA).

Material

Wortmannin and Mas7 were from Sigma (Sigma-Aldrich, Zwijndrecht, The Netherlands). Wortmannin was dissolved in DMSO (10 mM) and Mas7 in water (700 μM). Cell-free medium (CFM) was obtained spinning down 10 ml of cells at 3600 ***g*** for 5 min. Subsequently, supernatant was passed through a 0.22 μm filter yielding CFM. FM4-64 [*N*-(3-triethylammonium-propyl)-4-(6-(4-(diethylamino)phenyl)hexatrienyl) pyridinium dibromide; Invitrogen, Carlsbad CA, USA] was added to the cells to a final concentration of 4 ±M. After 5 min, the cells were washed once and immediately observed under the microscope.

Purification and lipid overlay assay of GST–YFP–2xFYVE

The YFP–2xFYVE fusion was transferred to the pGEX-KG vector and transformed into *E. coli* strain BL21(DE3). Expression was induced with 1 mM IPTG for 9 h at 20°C, and proteins were extracted using lysozyme and one round of freeze/thaw and sonication (Dowler *et al.*, 2000). GST–YFP–2xFYVE was purified using 1 ml GSTrap FF columns (Amersham Pharmacia Biosciences, Amersham, Buckinghamshire, UK). Pure protein was quantified and stored at −20°C until use in the protein lipid overlay assay. Determination of the phosphoinositide-binding properties of GST–YFP–2xFYVE was performed by the protein–lipid overlay assay, essentially as described by Dowler *et al.* (2000). All seven PPI isomers (18:1 CellSignals Inc., Lexington, KY, USA) were spotted onto a Hybond-C extra membrane (Amersham Pharmacia Biosciences) at various concentrations, and subsequently incubated with GST–YFP–2xFYVE fusion protein (0.5 μg ml^{-1}). Binding was detected using an anti-GST antibody (Santa Cruz Biotechnology Inc., Santa Cruz, CA, USA) and visualized by chemoluminescence.

Cowpea protoplast preparation and transfection

Cowpea (*V. unguiculata* L.) protoplasts were prepared from 10-day-old plants and transfected with 10 μg of plasmid DNA using the polyethylene glycol method as described by van Bokhoven *et al.* (1993).

Stable transformation of tobacco BY-2 cells and Arabidopsis plants

For single and double transformations of tobacco BY-2 cells, binary vectors were transformed into the *Agrobacterium tumefaciens* strain LBA4404. Bacteria were grown overnight. Next day, cultures were diluted to an OD_{600} of 0.25 and grown for 6 h at 28°C. Subsequently, 200 μl (or twice 100 μl in double transformations) of the *Agrobacterium* suspension plus acetosyringone, final concentration of 200 μM, was added to 8 ml of 4-day-old BY-2 cells in a Petri dish. After 3–5 days of incubation in the dark at 25°C, cells were washed twice with fresh medium and plated onto BY-2 agar plates, containing appropriate antibiotics for selection, and incubated further for another 3–4 weeks in the dark at 25°C. Positive calli, examined for fluorescence using a fluorescence stereo microscope, were transferred to a fresh BY-2 agar plate containing appropriate antibiotics. After 2 weeks, fluorescent calli were transferred to liquid BY-2 medium and sub-cultured weekly. *A. thaliana* cv. Columbia plants were transformed using *A. tumefaciens* strain EHA105, carrying pGreend35S::YFP–2xFYVE, using the standard floral dip method (Clough and Bent, 1998). Kanamycin-resistant T_2 plants were selected for fluorescence using a fluorescence stereomicroscope. Homozygous T_3 plants were used for microscopy. Seeds were vapour-sterilized and germinated on 0.5 × MS plates containing 1% agarose and 1% sucrose.

Confocal microscopy

BY-2 cells (4–5 days old) or protoplasts (17 h after transfection) were mounted in eight-chambered cover slides (Nalge Nunc International, Rochester, NY, USA). Arabidopsis seedlings were germinated for 3–4 days at 20°C and then transferred to object slides containing a fixed coverslide, separated by a spacer of approximately 0.32 mm. This created a microchamber to grow Arabidopsis seedlings (1–2 days in 0.5 × MS + 1% sucrose at 20°C) and could directly be used for microscopy. Fluorescence microscopy was performed using a Zeiss LSM 510 CLSM (confocal laser scanning microscope) (Carl-Zeiss GMBH, Jena, Germany), implemented on an inverted microscope (Axiovert 100, Carl-Zeiss GMBH, Jena, Germany). Excitation was provided by the 458, 488 and 514 nm Ar laser, 543 nm HeNe and 568 Kr lines controlled by an acousto-optical tuneable filter. Single- and dual-colour imaging were performed using single or dual excitation. For YFP/chlorophyll fluorescence, we used excitation/emission combinations of 514 nm/BP530–600 for YFP and LP650 for chlorophyll, in combination with the HFT458/514 primary, NFT635 secondary and NFT515 tertiary dichroic splitters. For YFP/FM4-64 dual scanning, the excitation/emission combinations of 488 nm/BP505–550 for YFP and 543 nm/LP650 for FM4-64 were used, in combination with the HFT488/543 primary, NFT570 secondary and NFT515 tertiary dichroic splitters. For CFP/YFP dual scanning, we used the excitation/emission combinations of 458 nm/BP470–500 for CFP and 514 nm/BP530–600 for YFP, in combination with the HFT458/514 primary, NFT635 secondary and NFT490 tertiary dichroic splitters. For YFP/mRFP dual scanning, we used the excitation/emission combinations of 488 nm/BP505–550 for YFP and 568 nm/LP585 for mRFP, in combination with the HFT488/568 primary, NFT570 secondary and NFT515 tertiary dichroic splitter. Cross-talk free images were acquired by operating the microscope in the multi-tracking mode. A Zeiss water-immersion C-Apochromat 40 × objective lens (NA 1.2), corrected for cover glass thickness, was used for scanning. Images were captured and analysed with ZEISS LSM510 software (version 3.2 SP3).

$^{32}P_i$ phospholipid labelling, extraction and analysis

BY-2 cells (4–5 days old, weekly sub-cultured) were pre-labelled with $^{32}PO_4^{3-}$ (carrier-free, Amersham Pharmacia Biosciences) for 3 h and subsequently treated by adding an equal volume of cell-free medium with or without either agonist or inhibitor at the indicated concentrations. Lipids were extracted, separated by thin layer chromatography, and quantified by phospho-imaging as described previously (den Hartog *et al.*, 2001; Munnik *et al.*, 1994a, 1996). PtdIns*3P* levels were determined by deacylating the lipid extract

with mono-methylamine and analysing the glycerophosphoinositides by anion-exchange HPLC as described previously (Meijer *et al.*, 2001; Munnik *et al.*, 1994a,b).

Acknowledgements

We thank Harald Stenmark, Jan Carette, Akihiko Nakano and Roger Tsien for kindly providing us with different constructs and Alan Musgrave for critical reading of the manuscript. This work was supported by the Council for Earth and Life Sciences (ALW), project number 810–66.012 (to J.E.M.V.) and 810–66.011 (to W.v.L.). Theodorus Gadella's lab was additionally supported by the EU Integrated Project on Molecular Imaging (LSHG-CT-2003–503259). Research in Teun Munnik's lab was supported by the Netherlands Organization for Scientific Research (NWO-ALW; numbers 813.06.0039, 863.04.004 and 864.05.001), the European Commission (HPRN-CT-2002–00251) and the Royal Netherlands Academy of Arts and Sciences (KNAW). A.M.L. was supported by a short-term EMBO fellowship. D.R.J. was supported by a EU–Marie Curie Individual Fellowship (HPMF-CT-2002–01218).

Supplementary Material

The following supplementary material is available for this article online:

Figure S1. Growth curve and morphological analysis of untransformed and YFP-2xFYVE transformed BY-2 cells.

Movie S1. YFP-2xFYVE dynamics in cowpea protoplasts.

Movie S2. YFP-2xFYVE dynamics in tobacco BY-2 cells.

Movie S3. Transient interactions between YFP-2xFYVE-labelled vesicles.

Movie S4 and S5. Movement of YFP-2xFYVE-labelled vesicles depend on the actin cytoskeleton.

Movie S6. Effect of wortmannin on YFP-2xFYVE localization.

Movie S7. Partial co-localization of YFP-2xFYVE with FM4-64.

Movie S8. YFP-2xFYVE labels endocytic/prevacuolar vesicles.

Movie S9. YFP-2xFYVE does not co-localize with STtmd-CFP.

Movie S10. YFP-2xFYVE dynamics in growing root hairs of Arabidopsis.

Movie S11. YFP-2xFYVE dynamics in leaf epidermal cells of Arabidopsis.

Movie S12. Image stack of a leaf epidermal cell.

Movie S13. YFP-2xFYVE dynamics in Arabidopsis guard cell.

Movie S14. Image stack of an Arabidopsis guard cell.

Movie S15. YFP-2xFYVE dynamics during cytokinesis in tobacco BY-2 cells.

Movie S16. Image stack of a dividing YFP-2xFYVE cell.

Movie S17. YFP-2xFYVE fluorescence is absent from the newly formed cell plate.

Movie S18. 4D-imaging of a dividing YFP-2xFYVE cell co-labelled with FM4-64.

This material is available as part of the online article from http://www.blackwell-synergy.com

References

Arcaro, A. and Wymann, M.P. (1993) Wortmannin is a potent phosphatidylinositol 3-kinase inhibitor: the role of phosphatidylinositol 3,4,5-trisphosphate in neutrophil responses. *Biochem J.* **296**, 297–301.

Behnia, R. and Munro, S. (2005) Organelle identity and the signposts for membrane traffic. *Nature*, **438**, 597–604.

Blondeau, F., Laporte, J., Bodin, S., Superti-Furga, G., Payrastre, B. and Mandel, J.L. (2000) Myotubularin, a phosphatase deficient in myotubular myopathy, acts on phosphatidylinositol 3-kinase and phosphatidylinositol 3-phosphate pathway. *Hum. Mol. Genet.* **9**, 2223–2229.

Boevink, P., Oparka, K., Santa Cruz, S., Martin, B., Betteridge, A. and Hawes, C. (1998) Stacks on tracks: the plant Golgi apparatus traffics on an actin/ER network. *Plant J.* **15**, 441–447.

van Bokhoven, H., Verver, J., Wellink, J. and van Kammen, A. (1993) Protoplasts transiently expressing the 200K coding sequence of the cowpea mosaic virus B-RNA support replication of M-RNA. *J. Gen. Virol.* **74**, 2233–2241.

Bolte, S., Talbot, C., Boutte, Y., Catrice, O., Read, N.D. and Satiat-Jeunemaitre, B. (2004) FM-dyes as experimental probes for dissecting vesicle trafficking in living plant cells. *J. Microsc.* **214**, 159–173.

Brown, R.A., Domin, J., Arcaro, A., Waterfield, M.D. and Shepherd, P.R. (1999) Insulin activates the alpha isoform of class II phosphoinositide 3-kinase. *J. Biol. Chem.* **274**, 14529–14532.

Burd, C.G. and Emr, S.D. (1998) Phosphatidylinositol(3)-phosphate signaling mediated by specific binding to RING FYVE domains. *Mol. Cell*, **2**, 157–162.

Clague, M.J. and Lorenzo, O. (2005) The myotubularin family of lipid phosphatases. *Traffic*, **6**, 1063–1069.

Clough, S.J. and Bent, A.F. (1998) Floral dip: a simplified method for *Agrobacterium*-mediated transformation of *Arabidopsis thaliana*. *Plant J.* **16**, 735–743.

Contento, A.L., Xiong, Y. and Bassham, D.C. (2005) Visualization of autophagy in Arabidopsis using the fluorescent dye monodansylcadaverine and a GFP-AtATG8e fusion protein. *Plant J.* **42**, 598–608.

Corvera, S., D'Arrigo, A. and Stenmark, H. (1999) Phosphoinositides in membrane traffic. *Curr. Opin. Cell Biol.* **11**, 460–465.

Das, S., Hussain, A., Bock, C., Keller, W.A. and Georges, F. (2005) Cloning of *Brassica napus* phospholipase C2 (BnPLC2), phosphatidylinositol 3-kinase (BnVPS34) and phosphatidylinositol synthase1 (BnPtdIns S1) – comparative analysis of the effect of abiotic stresses on the expression of phosphatidylinositol signal transduction-related genes in *B. napus*. *Planta*, **220**, 777–784.

DeWald, D.B., Torabinejad, J., Jones, C.A., Shope, J.C., Cangelosi, A.R., Thompson, J.E., Prestwich, G.D. and Hama, H. (2001) Rapid accumulation of phosphatidylinositol 4,5-bisphosphate and inositol 1,4,5-trisphosphate correlates with calcium mobilization in salt-stressed Arabidopsis. *Plant Physiol.* **126**, 759–769.

Dhonukshe, P., Baluska, F., Schlicht, M., Hlavacka, A., Samaj, J., Friml, J. and Gadella, T.W., Jr. (2006) Endocytosis of cell surface material mediates cell plate formation during plant cytokinesis. *Dev. Cell*, **10**, 137–150.

Dowler, S., Currie, R.A., Campbell, D.G., Deak, M., Kular, G., Downes, C.P. and Alessi, D.R. (2000) Identification of pleckstrin-homology-domain-containing proteins with novel phosphoinositide-binding specificities. *Biochem. J.* **351**, 19–31.

Duclos, S., Diez, R., Garin, J., Papadopoulou, B., Descoteaux, A., Stenmark, H. and Desjardins, M. (2000) Rab5 regulates the kiss and run fusion between phagosomes and endosomes and the acquisition of phagosome leishmanicidal properties in RAW 264.7 macrophages. *J Cell Sci.* **113** (Pt 19), 3531–3541.

Ellson, C.D., Anderson, K.E., Morgan, G., Chilvers, E.R., Lipp, P., Stephens, L.R. and Hawkins, P.T. (2001) Phosphatidylinositol 3-phosphate is generated in phagosomal membranes. *Curr. Biol.* **11**, 1631–1635.

Foster, F.M., Traer, C.J., Abraham, S.M. and Fry, M.J. (2003) The phosphoinositide (PI) 3-kinase family. *J. Cell Sci.* **116**, 3037–3040.

Frank, W., Munnik, T., Kerkmann, K., Salamini, F. and Bartels, D. (2000) Water deficit triggers phospholipase D activity in the resurrection plant *Craterostigma plantagineum*. *Plant Cell*, **12**, 111–124.

Gaullier, J.M., Simonsen, A., D'Arrigo, A., Bremnes, B., Stenmark, H. and Aasland, R. (1998) FYVE fingers bind PtdIns(3)P. *Nature*, **394**, 432–433.

Gaullier, J.M., Simonsen, A., D'Arrigo, A., Bremnes, B. and Stenmark, H. (1999) FYVE finger proteins as effectors of phosphatidylinositol 3-phosphate. *Chem. Phys. Lipids*, **98**, 87–94.

Gillooly, D.J., Morrow, I.C., Lindsay, M., Gould, R., Bryant, N.J., Gaullier, J.M., Parton, R.G. and Stenmark, H. (2000) Localization of phosphatidylinositol 3-phosphate in yeast and mammalian cells. *EMBO J.* **19**, 4577–4588.

den Hartog, M., Musgrave, A. and Munnik, T. (2001) Nod factor-induced phosphatidic acid and diacylglycerol pyrophosphate formation: a role for phospholipase C and D in root hair deformation. *Plant J.* **25**, 55–65.

Henry, R.M., Hoppe, A.D., Joshi, N. and Swanson, J.A. (2004) The uniformity of phagosome maturation in macrophages. *J. Cell Biol.* **164**, 185–194.

Herman, P.K. and Emr, S.D. (1990) Characterization of VPS34, a gene required for vacuolar protein sorting and vacuole segregation in *Saccharomyces cerevisiae*. *Mol. Cell. Biol.* **10**, 6742–6754.

Herman, P.K., Stack, J.H. and Emr, S.D. (1991) A genetic and structural analysis of the yeast Vps15 protein kinase: evidence for a direct role of Vps15p in vacuolar protein delivery. *EMBO J.* **10**, 4049–4060.

Hernandez, L.E., Escobar, C., Drobak, B.K., Bisseling, T. and Brewin, N.J. (2004) Novel expression patterns of phosphatidylinositol 3-hydroxy kinase in nodulated *Medicago* spp. plants. *J. Exp. Bot.* **55**, 957–959.

van Himbergen, J.A.J., ter Riet, B., Meijer, H.J.G., van den Ende, H., Musgrave, A. and Munnik, T. (1999) Mastoparan analogues stimulate phospholipase C- and phospholipase D-activity in *Chlamydomonas*: a comparative study. *J. Exp. Bot.* **50**, 1735–1742.

Hong, Z. and Verma, D.P. (1994) A phosphatidylinositol 3-kinase is induced during soybean nodule organogenesis and is associated with membrane proliferation. *Proc. Natl Acad. Sci. USA*, **91**, 9617–9621.

Jung, J.Y., Kim, Y.W., Kwak, J.M., Hwang, J.U., Young, J., Schroeder, J.I., Hwang, I. and Lee, Y. (2002) Phosphatidylinositol 3- and 4-phosphate are required for normal stomatal movements. *Plant Cell*, **14**, 2399–2412.

Kihara, A., Noda, T., Ishihara, N. and Ohsumi, Y. (2001) Two distinct Vps34 phosphatidylinositol 3-kinase complexes function in autophagy and carboxypeptidase Y sorting in *Saccharomyces cerevisiae*. *J. Cell Biol.* **152**, 519–530.

Kim, D.H., Eu, Y.J., Yoo, C.M., Kim, Y.W., Pih, K.T., Jin, J.B., Kim, S.J., Stenmark, H. and Hwang, I. (2001) Trafficking of phosphatidylinositol 3-phosphate from the trans-Golgi network to the lumen of the central vacuole in plant cells. *Plant Cell*, **13**, 287–301.

Klionsky, D.J. (2005) The molecular machinery of autophagy: unanswered questions. *J. Cell Sci.* **118**, 7–18.

Kotzer, A.M., Brandizzi, F., Neumann, U., Paris, N., Moore, I. and Hawes, C. (2004) AtRabF2b (Ara7) acts on the vacuolar trafficking pathway in tobacco leaf epidermal cells. *J. Cell Sci.* **117**, 6377–6389.

Kutateladze, T.G., Ogburn, K.D., Watson, W.T., de Beer, T., Emr, S.D., Burd, C.G. and Overduin, M. (1999) Phosphatidylinositol 3-phosphate recognition by the FYVE domain. *Mol. Cell*, **3**, 805–811.

Lee, G.J., Sohn, E.J., Lee, M.H. and Hwang, I. (2004) The Arabidopsis rab5 homologs rha1 and ara7 localize to the prevacuolar compartment. *Plant Cell Physiol.* **45**, 1211–1220.

van Leeuwen, W., Okresz, L., Bogre, L. and Munnik, T. (2004) Learning the lipid language of plant signalling. *Trends Plant Sci.* **9**, 378–384.

Meckel, T., Hurst, A.C., Thiel, G. and Homann, U. (2004) Endocytosis against high turgor: intact guard cells of *Vicia faba* constitutively endocytose fluorescently labelled plasma membrane and GFP-tagged K-channel KAT1. *Plant J.* **39**, 182–193.

Meijer, H.J.G., Divecha, N., van den Ende, H., Musgrave, A. and Munnik, T. (1999) Hyperosmotic stress induces rapid synthesis of phosphatidyl-D-inositol 3,4-bisphosphate in plant cells. *Planta*, **208**, 294–298.

Meijer, H.J., Berrie, C.P., Iurisci, C., Divecha, N., Musgrave, A. and Munnik, T. (2001) Identification of a new polyphosphoinositide in plants, phosphatidylinositol 5-monophosphate (PtdIns5P), and its accumulation upon osmotic stress. *Biochem. J.* **360**, 491–498.

Mueller-Roeber, B. and Pical, C. (2002) Inositol phospholipid metabolism in Arabidopsis. Characterized and putative isoforms of inositol phospholipid kinase and phosphoinositide-specific phospholipase C. *Plant Physiol.* **130**, 22–46.

Munnik, T., Irvine, R.F. and Musgrave, A. (1994a) Rapid turnover of phosphatidylinositol 3-phosphate in the green alga *Chlamydomonas eugametos*: signs of a phosphatidylinositide 3-kinase signalling pathway in lower plants? *Biochem. J.* **298**, 269–273.

Munnik, T., Musgrave, A. and de Vrije, T. (1994b) Rapid turnover of polyphosphoinositides in carnation flower petals. *Planta*, **193**, 89–98.

Munnik, T., de Vrije, T., Irvine, R.F. and Musgrave, A. (1996) Identification of diacylglycerol pyrophosphate as a novel metabolic product of phosphatidic acid during G-protein activation in plants. *J. Biol. Chem.* **271**, 15708–15715.

Munnik, T., Irvine, R.F. and Musgrave, A. (1998) Phospholipid signalling in plants. *Biochim. Biophys. Acta*, **1389**, 222–272.

Paciorek, T., Zazimalova, E., Ruthardt, N. *et al.* (2005) Auxin inhibits endocytosis and promotes its own efflux from cells. *Nature*, **435**, 1251–1256.

Park, K.Y., Jung, J.Y., Park, J., Hwang, J.U., Kim, Y.W., Hwang, I. and Lee, Y. (2003) A role for phosphatidylinositol 3-phosphate in abscisic acid-induced reactive oxygen species generation in guard cells. *Plant Physiol.* **132**, 92–98.

Parrish, W.R., Stefan, C.J. and Emr, S.D. (2004) Essential role for the myotubularin-related phosphatase Ymr1p and the synaptojanin-like phosphatases Sjl2p and Sjl3p in regulation of phosphatidylinositol 3-phosphate in yeast. *Mol. Biol. Cell*, **15**, 3567–3579.

Parrish, W.R., Stefan, C.J. and Emr, S.D. (2005) PtdIns(3)P accumulation in triple lipid-phosphatase-deletion mutants triggers lethal hyperactivation of the Rho1p/Pkc1p cell-integrity MAP kinase pathway. *J. Cell Sci.* **118**, 5589–5601.

Parton, R.M., Fischer-Parton, S., Trewavas, A.J. and Watahiki, M.K. (2003) Pollen tubes exhibit regular periodic membrane trafficking events in the absence of apical extension. *J. Cell Sci.* **116**, 2707–2719.

Pical, C., Westergren, T., Dove, S.K., Larsson, C. and Sommarin, M. (1999) Salinity and hyperosmotic stress induce rapid increases in phosphatidylinositol 4,5-bisphosphate, diacylglycerol pyrophosphate, and phosphatidylcholine in *Arabidopsis thaliana* cells. *J. Biol. Chem.* **274**, 38232–38240.

Roggo, L., Bernard, V., Kovacs, A.L., Rose, A.M., Savoy, F., Zetka, M., Wymann, M.P. and Muller, F. (2002) Membrane transport in *Caenorhabditis elegans*: an essential role for VPS34 at the nuclear membrane. *EMBO J.* **21**, 1673–1683.

Schu, P.V., Takegawa, K., Fry, M.J., Stack, J.H., Waterfield, M.D. and Emr, S.D. (1993) Phosphatidylinositol 3-kinase encoded by yeast VPS34 gene essential for protein sorting. *Science*, **260**, 88–91.

Shin, H.W., Hayashi, M., Christoforidis, S. *et al.* (2005) An enzymatic cascade of Rab5 effectors regulates phosphoinositide turnover in the endocytic pathway. *J. Cell Biol.* **170**, 607–618.

Simonsen, A., Wurmser, A.E., Emr, S.D. and Stenmark, H. (2001) The role of phosphoinositides in membrane transport. *Curr. Opin. Cell Biol.* **13**, 485–492.

Stack, J.H. and Emr, S.D. (1994) Vps34p required for yeast vacuolar protein sorting is a multiple specificity kinase that exhibits both protein kinase and phosphatidylinositol-specific PI 3-kinase activities. *J. Biol. Chem.* **269**, 31552–31562.

Stack, J.H., DeWald, D.B., Takegawa, K. and Emr, S.D. (1995a) Vesicle-mediated protein transport: regulatory interactions between the Vps15 protein kinase and the Vps34 PtdIns 3-kinase essential for protein sorting to the vacuole in yeast. *J. Cell Biol.* **129**, 321–334.

Stack, J.H., Herman, P.K., DeWald, D.B., Marcusson, E.G., Lin Cereghino, J., Horazdovsky, B.F. and Emr, S.D. (1995b) Novel protein kinase/phosphatidylinositol 3-kinase complex essential for receptor-mediated protein sorting to the vacuole in yeast. *Cold Spring Harb. Symp. Quant. Biol.* **60**, 157–170.

Stenmark, H. and Gillooly, D.J. (2001) Intracellular trafficking and turnover of phosphatidylinositol 3-phosphate. *Semin. Cell Dev. Biol.* **12**, 193–199.

Stenmark, H., Aasland, R., Toh, B.H. and D'Arrigo, A. (1996) Endosomal localization of the autoantigen EEA1 is mediated by a zinc-binding FYVE finger. *J. Biol. Chem.* **271**, 24048–24054.

Stephens, L., Hawkins, P.T. and Downes, C.P. (1989) Metabolic and structural evidence for the existence of a third species of polyphosphoinositide in cells: D-phosphatidyl-myo-inositol 3-phosphate. *Biochem. J.* **259**, 267–276.

Stephens, L., Cooke, F.T., Walters, R., Jackson, T., Volinia, S., Gout, I., Waterfield, M.D. and Hawkins, P.T. (1994) Characterization of a phosphatidylinositol-specific phosphoinositide 3-kinase from mammalian cells. *Curr. Biol.* **4**, 203–214.

Stromhaug, P.E., Reggiori, F., Guan, J., Wang, C.W. and Klionsky, D.J. (2004) Atg21 is a phosphoinositide binding protein required for efficient lipidation and localization of Atg8 during uptake of aminopeptidase I by selective autophagy. *Mol. Biol. Cell.* **15**, 3553–3566.

Takano, J., Miwa, K., Yuan, L., von Wiren, N. and Fujiwara, T. (2005) Endocytosis and degradation of BOR1, a boron transporter of *Arabidopsis thaliana*, regulated by boron availability. *Proc. Natl Acad. Sci. USA*, **102**, 12276–12281.

Taylor, G.S., Maehama, T. and Dixon, J.E. (2000) Inaugural article: myotubularin, a protein tyrosine phosphatase mutated in myotubular myopathy, dephosphorylates the lipid second messenger, phosphatidylinositol 3-phosphate. *Proc. Natl Acad. Sci. USA*, **97**, 8910–8915.

Ueda, T., Yamaguchi, M., Uchimiya, H. and Nakano, A. (2001) Ara6, a plant-unique novel type Rab GTPase, functions in the endocytic pathway of *Arabidopsis thaliana*. *EMBO J.* **20**, 4730–4741.

Vanhaesebroeck, B. and Waterfield, M.D. (1999) Signaling by distinct classes of phosphoinositide 3-kinases. *Exp. Cell Res.* **253**, 239–254.

Welters, P., Takegawa, K., Emr, S.D. and Chrispeels, M.J. (1994) AtVPS34, a phosphatidylinositol 3-kinase of *Arabidopsis thaliana*, is an essential protein with homology to a calcium-dependent lipid binding domain. *Proc. Natl Acad. Sci. USA*, **91**, 11398–11402.

Wurmser, A.E. and Emr, S.D. (1998) Phosphoinositide signaling and turnover: PtdIns(3)P, a regulator of membrane traffic, is transported to the vacuole and degraded by a process that requires lumenal vacuolar hydrolase activities. *EMBO J.* **17**, 4930–4942.

Wurmser, A.E. and Emr, S.D. (2002) Novel PtdIns(3)P-binding protein Etf1 functions as an effector of the Vps34 PtdIns 3-kinase in autophagy. *J. Cell Biol.* **158**, 761–772.

Xiong, Y., Contento, A.L. and Bassham, D.C. (2005) AtATG18a is required for the formation of autophagosomes during nutrient stress and senescence in *Arabidopsis thaliana*. *Plant J.* **42**, 535–546.

Zerial, M. and McBride, H. (2001) Rab proteins as membrane organizers. *Nature Rev. Mol. Cell Biol.* **2**, 107–117.

Zerial, M. and Stenmark, H. (1993) Rab GTPases in vesicular transport. *Curr. Opin. Cell Biol.* **5**, 613–620.

Zhang, J., Banfic, H., Straforini, F., Tosi, L., Volinia, S. and Rittenhouse, S.E. (1998) A type II phosphoinositide 3-kinase is stimulated via activated integrin in platelets. A source of phosphatidylinositol 3-phosphate. *J. Biol. Chem.* **273**, 14081–14084.

Zheng, H., Camacho, L., Wee, E., Batoko, H., Legen, J., Leaver, C.J., Malho, R., Hussey, P.J. and Moore, I. (2005) A Rab-E GTPase mutant acts downstream of the Rab-D subclass in biosynthetic membrane traffic to the plasma membrane in tobacco leaf epidermis. *Plant Cell*, **17**, 2020–2036.

